Journal of Magnetic Resonance 210 (2011) 90–97

Contents lists available at ScienceDirect

Journal of Magnetic Resonance

journal homepage: www.elsevier.com/locate/jmr

Accelerating multi-echo T2 weighted MR imaging: Analysis prior group-sparse optimization

Angshul Majumdar *, Rabab K. Ward

Department of Electrical and Computer Engineering, University of British Columbia, Canada

ARTICLE INFO

Article history:
Received 8 October 2010
Revised 10 February 2011
Available online 18 February 2011

Keywords:
Compressed Sensing
Optimization
Image reconstruction

ABSTRACT

This works addresses the problem of reconstructing multi-echo T2 weighted MR images from partially sampled K-space data. Previous studies in reconstructing MR images from partial samples of the K-space used Compressed Sensing (CS) techniques to exploit the spatial correlation of the images (leading to sparsity in transform domain). Such techniques can be employed to reconstruct the individual T2 weighted images. However, in the current context, the different images are not independent; they are images of the same cross section, and hence are highly correlated. In this work, we not only exploit the spatial correlation within the image, but also the correlation between the images to achieve even better reconstruction results.

For individual MR images, CS based techniques lead to a sparsity promoting optimization problem in a transform domain. In this paper, we show how to extend the same framework in order to incorporate correlation between images leading to group sparsity promoting optimization. Group sparsity promoting optimization is popularly formulated as a synthesis prior problem. The synthesis prior formulation for group sparsity leads to superior reconstruction results compared to ordinary sparse reconstruction. However, in this paper we show that when group sparsity is framed as an analysis prior problem the reconstruction results are even better for proper choice of the sparsifying transform.

An interesting observation of this work is that when the same sampling pattern is used to sample the K-space for all the T2 weighted echoes, group sparsity does not yield any noticeable improvement, but when different sampling patterns are used for different echoes, our proposed group sparsity promoting formulation yields significant improvement (in terms of Normalized Mean Squared Error) over previous CS based techniques.

1. Introduction

In T2 weighted Magnetic Resonance Imaging (MRI), multiple echoes of the same anatomical slice with varying echo times are acquired. The objective is to reconstruct the multi-echo T2 weighted MR images. Generally this kind of data is acquired for computing T2 maps.

In conventional MR imaging the echoes are acquired by fully sampling the K-space on a rectangular grid and applying 2D inverse Fast Fourier Transform to reconstruct the image. Such conventional K-space sampling methods become prohibitively slow for practical multi-echo T2 weighted MR imaging, e.g. acquiring 32 echoes of a while imaging a single slice of the rat's spinal cord using Carr Purcell Meiboom Gill (CPMG) sequence takes about 40 min. In this paper, we look how to reduce this data acquisition time for such multi-echo T2 weighted MRI.

For single 2D MR images the scan time can be reduced by randomly acquiring only a subset of all the K-space lines in frequency encoding direction. The images from such partially sampled K-space data can be reconstructed by using Compressed Sensing (CS) based techniques [1,2]. CS techniques utilize spatial correlation (leading to sparsity of the image in a transform domain) in the MR image in order to reconstruct it.

Such a CS technique can be directly applied to each of the echoes of the multiple T2 weighted images. However, this is not the best possible approach. The multiple T2 weighted images are correlated with each other. In this work, we propose to exploit both intra-image spatial correlation as well as inter-image correlation to achieve even better reconstruction. This too will be a CS based formulation, but instead of reconstructing each image individually, we will jointly reconstruct all the T2 weighted images simultaneously. Our formulation to the joint reconstruction problem will lead to group-sparse optimization. The improvement in reconstruction is not achieved when a fixed K-space sampling pattern

* Corresponding author. Address: Kaiser 2010, 2332 Main Mall, Vancouver, BC, Canada V6T 1Z4.

E-mail addresses: angshulm@ece.ubc.ca (A. Majumdar), rababw@ece.ubc.ca (R.K. Ward).

1090-7807/$ - see front matter © 2011 Elsevier Inc. All rights reserved.
doi:10.1016/j.jmr.2011.02.015

is used for all the echoes, but is achieved when different sampling patterns are used for each echo.

In recent times there have been several attempts to improve computation of T2 maps. In [3], the goal was to find an empirical dictionary that would be better at sparsifying the MR images than the mathematical ones like wavelets, curvelets or contourlets. They applied this learned dictionary technique for computing the T2 map. In [4], the problem was to compute T2 maps from radial K-space scans. The focus of this work is different from both of these. We use a standard wavelet dictionary for the sparsifying transform. Instead of using radial scanning, we employ Cartesian scans. Acceleration is achieved by randomly omitting scan lines along the y-axis.

The main goal of this work is to accelerate the MRI scan by partially sampling the K-space. Creating the T2 maps from the MR images is a non-linear operation. However, it is fair to assume that if the MR images can be reconstructed fairly accurately from the partial K-space scans, the T2 map obtained from these images will be close to the ones corresponding to full K-space scans. This work shows that the assumption is valid and the T2 maps generated from these MR images (from partial K-space scans) are fairly accurate (compared to the T2 map generated from the full K-space).

This work discusses the joint reconstruction problem in the context of multi-echo T2 weighted MR imaging. However the techniques developed in this paper are applicable to T1 weighted MR imaging as well. The rest of the paper is organized into several sections. The theoretical development behind the group-sparse optimization is described in the following section. The experimental results are in Section 3. The conclusions of this work are discussed in Section 4.

2. Reconstruction of T2 weighted images

Contrast between various tissues in the MR image is dependent on the T2 weighting, i.e. for a particular T2 weighting the contrast between two tissues A and B may be high, while for another T2 weighting the contrast may be low. In multi-echo T2 weighted imaging each image varies from the other in their contrast between the tissues. Since all the T2 weighted images actual correspond to the same cross section, they are highly correlated amongst themselves.

In this section, first we will discuss the theory behind the reconstruction of single 2D MR images from partially sampled K-space data. CS techniques exploit the spatial correlation within the MR images in order to reconstruct them from reduced number of K-space samples. Later we will show how to exploit the correlation between the images along with spatial correlation to achieve better reconstruction of multi-echo T2 weighted MR images.

2.1. Reconstructing single MR images

The partially sampled K-space data acquisition model for the underlying image can be expressed as,

$$y_{m\times 1} = R_{m\times N^2} F_{N^2\times N^2} x_{N^2\times 1} + \eta_{m\times 1}, \quad m \leqslant N^2 \tag{1}$$

where y is the acquired K-space samples, x is the underlying image in vectorized form, F is the Fourier transform, R is the restriction operator (mask) that chooses the sampling positions and η is white Gaussian noise.

The inverse problem (1) is under-determined and hence does not have a unique solution. To reconstruct the underlying image, some prior information regarding it is necessary. Many Compressed Sensing based MR reconstruction techniques [1,2,5,6] assume that the image to be reconstructed is approximately sparse in some transform domain (wavelet, contourlet, finite difference). In this work, we are mainly interested in wavelets as the sparsifying transform.

The wavelet analysis and synthesis equations are:

$$\text{Analysis} : \alpha = Wx \tag{2a}$$

$$\text{Synthesis} : x = W^T\alpha \tag{2b}$$

The wavelet coefficients in α are approximately s-sparse, i.e. only s coefficients are non-zeroes while the rest are zeroes or very close to zero. Typically, for MR images, around 5–10% of the coefficients have significant values. We are interested in those wavelet families that are either orthogonal ($W^TW = I = WW^T$), in that case the dimensionality of the original image and the transform coefficients is the same, or are redundant (tight-frames: $W^TW = I \neq WW^T$), in that case the dimensionality of the wavelet coefficients is larger.

Incorporating the wavelet coefficients into (1),

$$y = RFW^T\alpha + \eta \tag{3}$$

In Compressed Sensing (CS), instead of solving the image directly the wavelet coefficient of the image is solved from (3). CS aims at recovering only the s high valued wavelet coefficients. The coefficients that are close to zero are indistinguishable from noise and hence can not be recovered.

In the pixel domain, an $N \times N$ image under consideration has N^2 unknowns. However the pixel values are highly correlated locally. The wavelet transform effectively 'whitens' the image by removing the spatial correlations [7]. This leaves s nearly independent high valued wavelet coefficients.

The inverse problem (10) has effectively only $2s$ unknowns – s positions and s values. Intuitively, solving for these $2s$ unknowns will require far less number of equations than solving for the image directly which has N^2 unknowns. CS based recovery algorithms solves for the sparse wavelet transform coefficients by solving the following optimization problem,

$$\min_{\alpha} \|\alpha\|_1 \text{ subject to } \|y - RFW^T\alpha\|_2 \leqslant \sigma \tag{4}$$

where σ is proportional to the standard deviation of noise, $\|.\|_1$ is the sum of absolute values of the coefficients in the vector and $\|.\|_2$ is the square root of the sum of squared values of the coefficients in the vector.

Now in order to get a reasonably good estimate of the signal via l_1-minimization, the number of K-space samples needed is [8],

$$m = O\left(s\log\frac{N^2}{s}\right) \tag{5}$$

Once the wavelet coefficients are recovered, the image is reconstructed by applying the wavelet synthesis Eq. (2b).

2.2. Group-sparse reconstruction of T2 weighted images

As mentioned earlier, in T2 weighted imaging one acquires multiple images of the same cross section by varying the echo time. Assume, K-space data for T such weightings have been acquired. This is represented by,

$$y_i = R_iFx_i + \eta_i, \quad i = 1,\ldots,T \tag{6}$$

where R_i represents that we can have a different sampling pattern for each T2 weighting.

The problem is to reconstruct the T2 weighted images (x_i's) given their K-space samples (y_i's).

A straightforward application of CS will repeatedly apply (4) to reconstruct the T2 weighted individually (for each i). In this work, we aim at joint reconstruction of all the T2 weighted images. How-

ever, such a formulation does not account for inter-image correlation. To reconstruct the images simultaneously using both intra-image spatial correlation as well as inter-image correlation in order to improve reconstruction accuracy we propose this work.

Incorporating the wavelet transform, (6) can be expressed concisely as follows,

$$\begin{bmatrix} y_1 \\ \cdots \\ y_T \end{bmatrix} = \begin{bmatrix} R_1 F W^T & 0 & 0 \\ 0 & \cdots & 0 \\ 0 & 0 & R_T F W^T \end{bmatrix} \begin{bmatrix} \alpha_1 \\ \cdots \\ \alpha_T \end{bmatrix} + \begin{bmatrix} \eta_1 \\ \cdots \\ \eta_T \end{bmatrix} \quad \text{or,} \quad \tilde{y} = \Phi\tilde{\alpha} + \tilde{\eta} \tag{7}$$

$$\text{where } \tilde{y} = \begin{bmatrix} y_1 \\ \cdots \\ y_T \end{bmatrix}, \quad \Phi = \begin{bmatrix} R_1 F W^T & 0 & 0 \\ 0 & \cdots & 0 \\ 0 & 0 & R_T F W^T \end{bmatrix},$$

$$\tilde{\alpha} = \begin{bmatrix} \alpha_1 \\ \cdots \\ \alpha_T \end{bmatrix} \quad \text{and} \quad \tilde{\eta} = \begin{bmatrix} \eta_1 \\ \cdots \\ \eta_T \end{bmatrix}$$

The wavelet transform effectively encodes the edges in an image. When the edge is more pronounced the wavelet coefficients are high. When the edge is not so sharp, the wavelet coefficients are low. In smooth areas the wavelet coefficients are zero. The following toy example illustrates the fact.

Consider a small image matrix with sharp boundary for a particular T2 weighting (Fig. 1a). The 0's correspond to tissue *B* and the 1's correspond to tissue *W*. The wavelet transform (Fig. 1b.) captures the vertical discontinuity between *W*–*B*. The values in the last column should be ignored, the wavelet transform assumes that the signal is periodic and computes the boundary between *B* and *W*.

Fig. 1 shows that when the tissue boundary is pronounced, the wavelet transform along the boundary is high. Now consider a different value of T2 weighting, such that the contrast between *W* and *B* is less pronounced (Fig. 2a). The wavelet transform of this matrix is shown in Fig. 2b. We can see now that even though the position of the high valued transform coefficients is the same, their values have changed. As the contrast has reduced, the value of the wavelet coefficients has reduced.

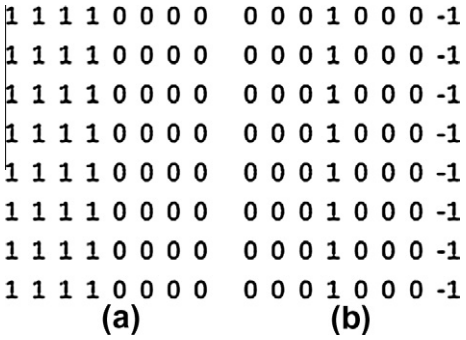

Fig. 1. First T2 weighting: (a) tissue boundary; (b) wavelet coefficients.

This example is to corroborate the fact that as long as the anatomy of the brain slice does not change, the positions of the high valued wavelet transform coefficients will not change for different T2 weightings. Mathematically, this means that there should be a high degree of mutual correlation between the wavelet transforms of any two T2 weighted images of the same anatomical cross section. Fig. 3. shows the scatter plot between the wavelet coefficients of two randomly chosen T2 weighted images of rat's spinal cord. The plot shows that the correlation is almost linear.

The linear relationship, corroborates our physical understanding of the fact that wavelet coefficients of two T2 weighted images have similar valued coefficients at similar positions.

The wavelet coefficient vector for each image (α_i) in (7) corresponding to different T2 weightings are of length N^2 (assuming for the time being the wavelet transform we are considering is orthogonal). The $\tilde{\alpha}$ in (7) can be grouped according to their positions as shown in Fig. 4. We will have N^2 groups (same as the number of wavelet coefficients for each image) and within each group there will be T (same as the total number of T2 weightings) coefficients.

We have argued why the wavelet coefficients should have similar values at similar positions. It is known that the wavelet transform leads to a sparse representation of the individual MR images. If each α_i's are approximately s-sparse, then following the argu-

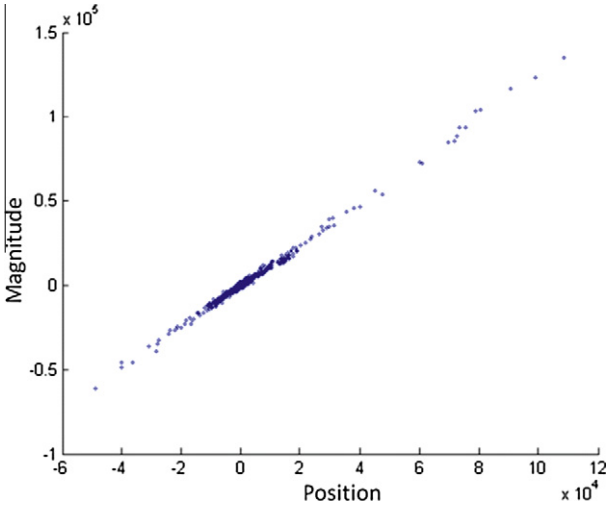

Fig. 3. Scatter plot of wavelet coefficients of two T2 weighted images of rat's spinal cord.

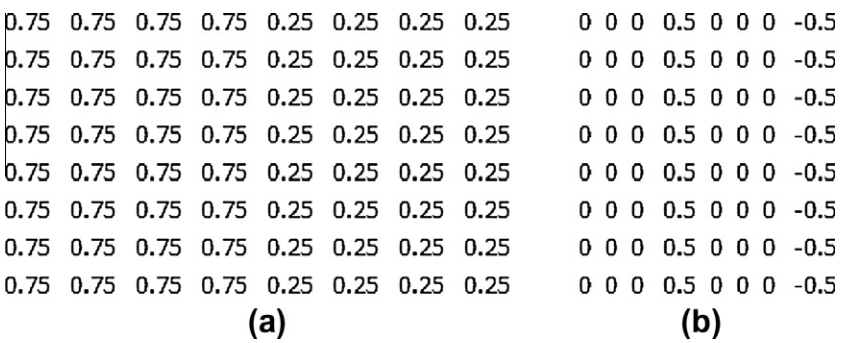

Fig. 2. Second T2 weighting: (a) tissue boundary; (b) wavelet coefficients.

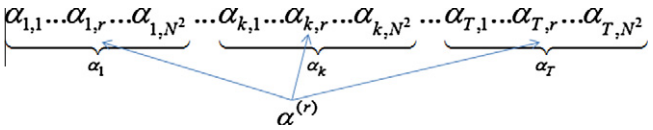

Fig. 4. Grouping of wavelet coefficients according to their position.

ment that different α_i's will have high valued coefficients at similar positions, we can say that the vector $\tilde{\alpha}$ is going to be approximately s-group sparse, i.e. there are approximately only s groups that have high valued wavelet coefficients and rest of the groups have zero coefficients or coefficients close to zero.

Therefore one needs to incorporate group sparsity into the optimization problem. There have been previous studies [9–11] that proposed the following mixed $l_{2,1}$-minimization for solving the group sparsity promoting optimization problem,

$$\min_{\tilde{\alpha}} \|\tilde{\alpha}\|_{2,1} \text{ subject to } \|\tilde{y} - \Phi\tilde{\alpha}\|_2 \leqslant \sigma \tag{8}$$

where $\|\tilde{\alpha}\|_{2,1} = \sum_{r=1}^{N^2}\left(\sum_{k=1}^{T}\alpha_{k,r}^2\right)^{1/2}$.

The l_2-norm $\left(\sum_{k=1}^{T}\alpha_{k,r}^2\right)^{1/2}$ over the group of correlated coefficients enforces the selection of the entire group of coefficients, whereas the summation over the l_2-norm enforces group sparsity, i.e. the selection of only a few groups. This problem can be solved with standard packages like Spectral Projected Gradient L1 [15]. Although group-sparse optimization is being introduced for the first time in MR image reconstruction, it has been used (with slightly different measures on group sparsity) previously in color imaging [12–14].

2.3. Benefit of group-sparse reconstruction

In the problem of reconstruction of T2 weighted images by sparse optimization, l_1-minimization is employed. It is assumed that each of the T2 weighted images is approximately s-sparse; and there are T such weighted images; therefore the full vector consisting of wavelet coefficients from all images$\tilde{\alpha}$ is approximately T s-sparse. Application of l_1-minimization requires about $M_1 = O\left(Ts\log\frac{N^2}{s}\right)$ K-space samples.

However, we have argued that $\tilde{\alpha}$ is actually s-group sparse. Compared to simple sparsity promoting optimization (l_1-minimization) we are exploiting more structure (the knowledge that the vector is sparse in groups). This information benefits reconstruction in the sense that in order to retrieve the same number of coefficients by $l_{2,1}$-minimization (8) the number of measurements required is only $M_{2,1} = O\left(Ts + s\log\frac{N^2}{s}\right)$ [16]. This is significantly less than the number of measurements required by simple sparsity based optimization.

Thus we expect to achieve the same level of reconstruction accuracy, but with lesser number of K-space samples when by our proposed group/row sparsity based reconstruction of T2 maps compared to simple sparsity based optimization. Or in other words, with the same number of K-space samples group sparsity based methods will yield better reconstruction results.

2.4. Group-sparse analysis prior formulation

The formulation in (8) is called the 'synthesis prior' formulation since it solves for the wavelet transform coefficients. Alternately we can formulate it as an 'analysis prior' formulation, where one can directly solve for the images. Instead of (7), we can express the combined data acquisition model for all the T2 weighted images as follows:

$$\begin{bmatrix} y_1 \\ \cdots \\ y_T \end{bmatrix} = \begin{bmatrix} R_1F & 0 & 0 \\ 0 & \cdots & 0 \\ 0 & 0 & R_TF \end{bmatrix}\begin{bmatrix} x_1 \\ \cdots \\ x_T \end{bmatrix} + \begin{bmatrix} \eta_1 \\ \cdots \\ \eta_T \end{bmatrix} \quad \text{or,} \quad \tilde{y} = \Psi\tilde{x} + \tilde{\eta} \tag{9}$$

where $\tilde{y} = \begin{bmatrix} y_1 \\ \cdots \\ y_T \end{bmatrix}$, $\Psi = \begin{bmatrix} R_1F & 0 & 0 \\ 0 & \cdots & 0 \\ 0 & 0 & R_TF \end{bmatrix}$, $\tilde{x} = \begin{bmatrix} x_1 \\ \cdots \\ x_T \end{bmatrix}$ and $\tilde{\eta} = \begin{bmatrix} \eta_1 \\ \cdots \\ \eta_T \end{bmatrix}$

Instead of employing a synthesis prior optimization as in (8), we propose the following group sparsity promoting analysis prior optimization:

$$\min_{\tilde{x}} \|H\tilde{x}\|_{2,1} \text{ subject to } \|\tilde{y} - \Psi\tilde{x}\|_2 \leqslant \sigma \tag{10}$$

where $H = \begin{bmatrix} W & 0 & 0 \\ 0 & \cdots & 0 \\ 0 & 0 & W \end{bmatrix}$

The synthesis prior (16) and the analysis prior (17) formulations are the same for orthogonal wavelets ($W^TW = I = WW^T$), but not for redundant wavelets $W^TW = I \neq WW^T$. The synthesis prior formulation is more popular in signal processing and machine learning. However, in a recent work [15], the following observations have been noted regarding analysis and synthesis prior reconstruction for sparse (not group-sparse) signals:

- For orthogonal wavelets both analysis and synthesis prior yield the same results (theoretically).
- Redundant wavelets with synthesis prior the results are worse than orthogonal wavelets.
- Redundant wavelets with analysis prior yield the best results.

In [17], the results were concluded for synthetic signals. We experimentally showed that similar conclusions can be drawn for sparsity based MR image reconstruction [18]. Following our previous work [18], instead of employing synthesis prior optimization we propose employing analysis prior group-sparse optimization to achieve even better reconstruction results. Unfortunately, there is no algorithm available for solving this problem (10).

3. Experimental results

The experimental evaluation was carried out on ex-vivo and in-vivo T2 weighted images of a rat's spinal cord. The data were collected with a 7T MRI scanner. The original ground-truth data consisted of a series of 16 fully-sampled echoes acquired with a CPMG sequence with increasing echo time (first echo was acquired with 13.476 ms echo time, and consecutive echoes with the echo spacing of 13.476 ms).

In this work, we simulate partial sampling of the K-space by randomly omitting lines in the frequency encoding direction. Three sampling patterns for 32, 48 and 64 lines in the read-out direction are shown below. They correspond to sampling ratios 12.5%, 18.75% and 25% of the full K-space. For all the sampling patterns, a third of the total sampling lines are used to densely sample the center of the K-space.

For reconstruction of individual T2 weighted images, different CS optimization can be used. One can apply (4) [2], or else one can apply Total Variation (TV) minimization [19]. However, the best results are obtained when both wavelet transform and TV is

combined to reconstruct the image via the following optimization [1,20].

$$\min_{\alpha} \|\alpha\|_1 + TV(W^T\alpha) \text{ subject to } \|y - RFW^T\alpha\|_2 \leqslant \sigma \quad (11)$$

This problem (11) is solved via the algorithm outlined in [21]. For the group-sparse synthesis prior optimization we employ the SPGL1 algorithm [15]. Algorithm for group-sparse analysis prior did not exist previously and hence we developed it in this work. The algorithm derived in the appendix will used for the purpose.

We will show that better results can be obtained by jointly reconstructing all the T2 weighted images. The joint reconstruction exploits group sparsity as outlined in this paper. We show the results for both synthesis prior with orthogonal wavelets and analysis prior with redundant wavelets. As we mentioned earlier, both the synthesis prior and the analysis prior are theoretically the same for orthogonal wavelets, hence we provide results for only synthesis prior. The results for synthesis prior with redundant wavelets are worse compared to the others, therefore we do not show these results as well. Unless otherwise mentioned in this work 'Group-sparse synthesis' employs orthogonal wavelets and 'Group-sparse analysis' employs redundant wavelets.

3.1. Quantitative evaluation

In this work, we experimented with several wavelet families (Haar, Daubechies, Coiflets, Symlets and Fractional Spline) as the sparsifying transform. The best results were obtained by Daubechies 6 wavelets at three levels of decomposition. In this work, we therefore report the results for this wavelet. The metric for quantitative comparison is the Normalized Mean Squared Error (NMSE) between the ground-truth and the reconstructed 16 images. Later, the difference image (between original and reconstructed) is provided for qualitative evaluation. In the following tables, 'Same sampling for all weighting' indicates that the same sampling pattern has been used for all the T2 weighted echoes where as 'Different sampling for each weighting' indicates that for each echo a different random sampling pattern has been used.

The following conclusions can be drawn from Tables 1 and 2:

- When the same sampling pattern is used for all the echoes, group sparsity promoting optimization does not yield any significant improvement over previously proposed technique [1,21]. But when different sampling patterns are used, the results from group-sparse optimization show significant improvement.
- The analysis prior optimization always yields significantly better results than the synthesis prior.

The T2 maps were computed from the reconstructed images (partial K-space scan) and were compared with the T2 map computed from the ground-truth (full K-space scan). The quantitative results are shown in Tables 3 and 4.

Table 1
NMSE for ex-vivo reconstructed images.

Reconstruction method	Same sampling for all weighting			Different sampling for each weighting		
	32	**48**	**64**	**32**	**48**	**64**
SparseMRI [1,21]	0.2703	0.2063	0.1845	0.2707	0.1970	0.1621
Group-sparse synthesis	0.2573	0.1923	0.1723	0.2320	0.1729	0.1422
Group-sparse analysis	0.2262	0.1659	0.1506	0.2002	0.1484	0.1241

Table 2
NMSE for in-vivo reconstructed images.

Reconstruction method	Same sampling for all weighting			Different sampling for each weighting		
	32	**48**	**64**	**32**	**48**	**64**
SparseMRI [1,21]	0.3775	0.1961	0.1374	0.3872	0.2446	0.1548
Group-sparse synthesis	0.3622	0.1952	0.1266	0.2907	0.1539	0.0963
Group-sparse analysis	0.3176	0.1708	0.1125	0.2443	0.1363	0.0840

Table 3
NMSE for ex-vivo T2 maps.

Reconstruction method	Same sampling for all weighting			Different sampling for each weighting		
	32	**48**	**64**	**32**	**48**	**64**
SparseMRI [1,21]	0.2777	0.2339	2158	0.3361	0.2350	0.1736
Group-sparse synthesis	0.2732	0.2086	0.1778	0.2648	0.1832	0.1623
Group-sparse analysis	0.2642	0.1934	0.1667	0.2288	0.1741	0.1437

Table 4
NMSE for in-vivo T2 maps.

Reconstruction method	Same sampling for all weighting			Different sampling for each weighting		
	32	**48**	**64**	**32**	**48**	**64**
SparseMRI [1,21]	0.4295	0.2325	0.1460	0.3899	0.2591	0.1731
Group-sparse synthesis	0.4212	0.2039	0.1388	0.3322	0.1702	0.1037
Group-sparse analysis	0.3754	0.1792	0.1161	0.2682	0.1510	0.0923

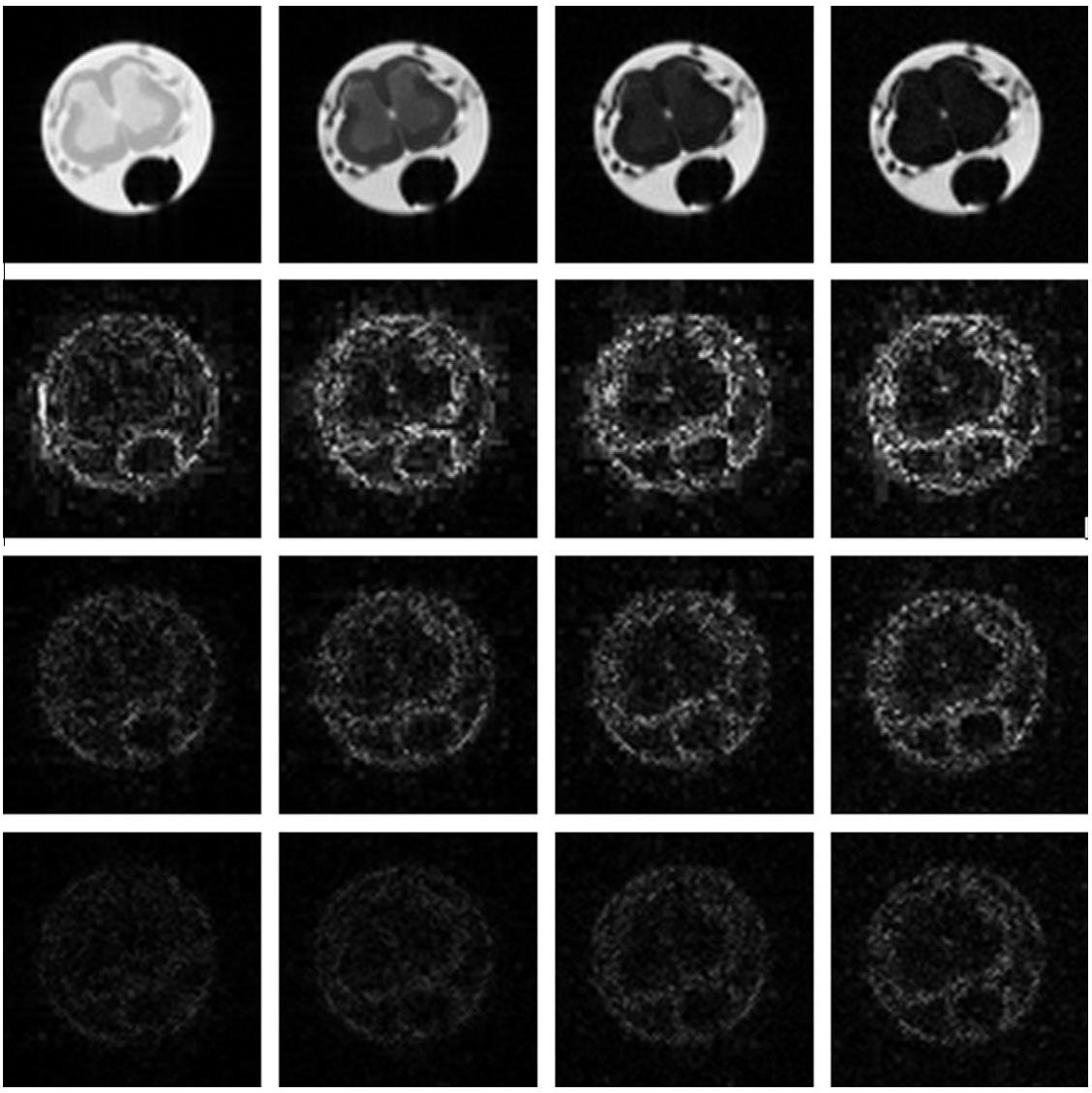

Fig. 5. Ex-vivo data. Top row – ground-truth images, echoes 1, 5, 9 and 13. Next three rows – corresponding difference images from SparseMRI, group-sparse synthesis prior and group-sparse analysis prior reconstruction.

3.2. Qualitative evaluation

Even though the NMSE values show significant improvement of our proposed technique over existing ones, they may not be the best indicators of image quality. For a qualitative comparison, we provide the difference images (= original − reconstructed) for the three different reconstruction techniques for 64 sampling lines. For each echo a new sampling pattern is used for acquiring K-space data. For scarcity of space we only show the results for ex-vivo data. It is not possible to provide all the sixteen images for each reconstruction algorithm, therefore we only show difference images for the following echoes – 1, 5, 9 and 13. For better visual clarity, the intensity of the difference images is magnified five times.

The difference images (Fig. 5) conclusively establish the superiority of our proposed technique over state-of-the-art CS based techniques in MR image reconstruction from partially sampled K-space data for T2 weighted images.

The difference images show how good the reconstruction is with respect to the ground-truth. However the end-users of MRI are more interested in the visual quality of the reconstructed image. For this reason, we provide the reconstructed images (Fig. 6) from the different methods for visual comparison. It is evident that our proposed method yields the best results.

We assume that if the MR images reconstructed from partial K-space scans are similar to those from full K-space scans, the corresponding T2 maps will be similar as well. This is a valid assumption. In Fig. 7, we show the T2 maps for the ex-vivo and in-vivo data. For the in-vivo data, only the portion corresponding to the spinal cord is fit. As can be seen, the result from our proposed method is very close to the one obtained from the full K-space scan.

4. Conclusion

In multi-echo T2 imaging, multiple T2 weighted K-space scans of the same cross section are obtained by varying the echo time. The challenge is to reduce the overall scan time. The reduction in scan time can be achieved by partially sampling the K-space. Thus from a signal processing perspective, the problem is to reconstruct the T2 weighted images from their partially sampled K-space data.

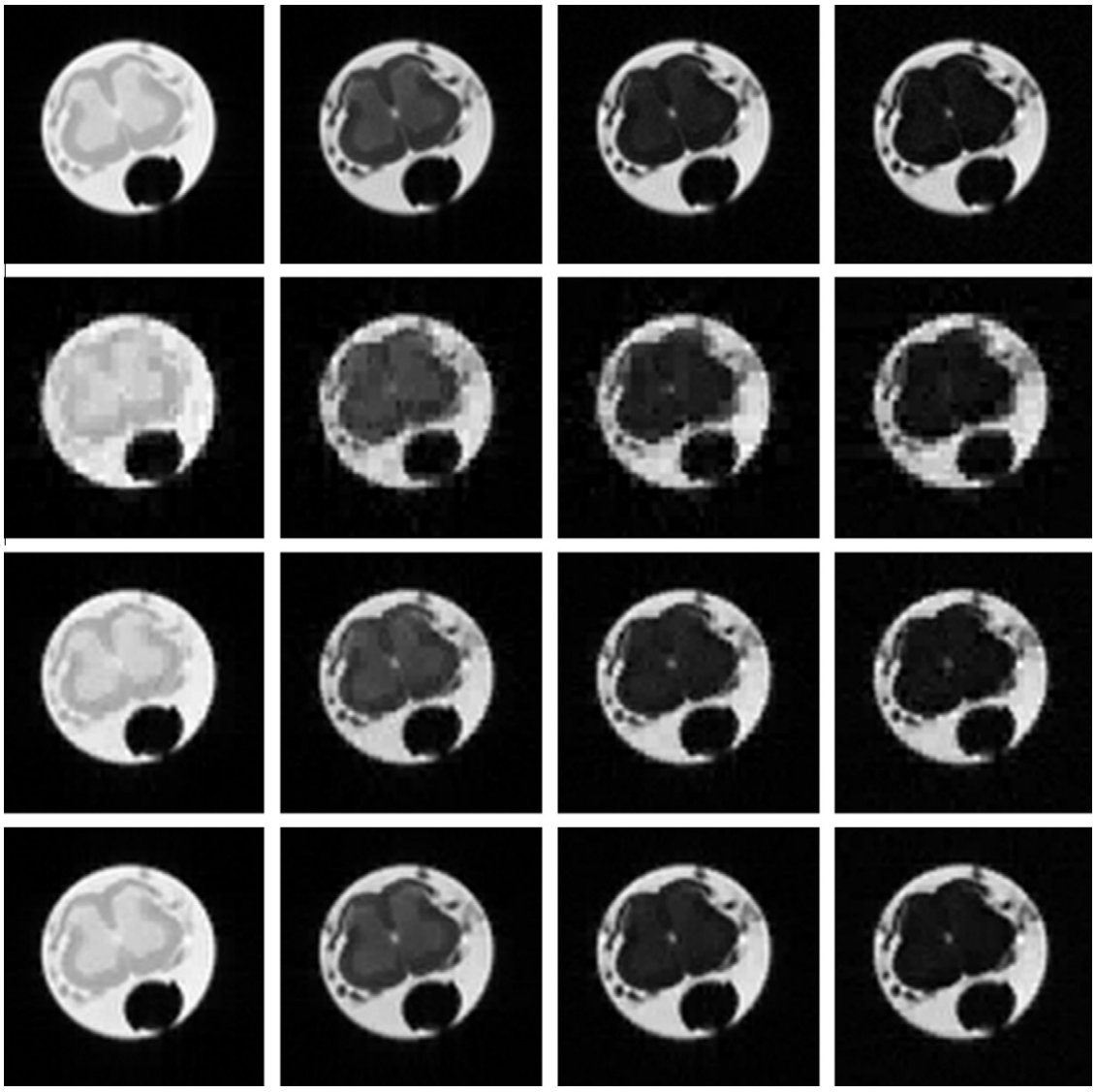

Fig. 6. Ex-vivo data. Top row – ground-truth images, echoes 1, 5, 9 and 13. Next three rows – corresponding reconstructed images from SparseMRI, group-sparse synthesis prior and group-sparse analysis prior reconstruction.

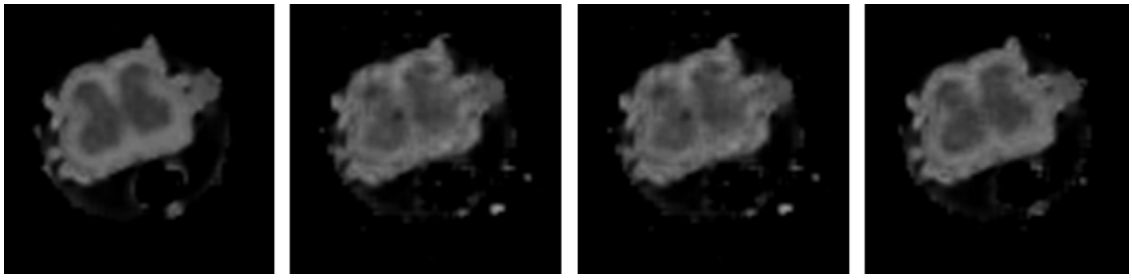

Fig. 7. T2 maps for ex-vivo (top) and in-vivo (bottom) data; from left to right – ground-truth, SparseMRI, group-sparse synthesis prior and group-sparse analysis prior reconstruction.

Research in Compressed Sensing (CS) based MR image reconstruction techniques have shown that it is possible to reconstruct individual MR images from their partial K-space measurements fairly accurately by exploiting their spatial correlation (sparsity of the images in a transform domain). It is possible to apply existing CS reconstruction techniques to the individual T2 weighted scans in order to reconstruct the corresponding images separately.

The aforesaid approach does not yield the best possible results. In this work, we show that instead of reconstructing the images individually by only exploiting their spatial correlation (transform domain sparsity) better results can be achieved when further information regarding the correlation amongst the different T2 weighted images is utilized as well. This approach gives improved results when different scanning patterns are used for acquiring K-

space scans for different T2 weightings. Most commercial scanners can be programmed to satisfy this condition. However, if the scanner can only acquire data from a fixed sampling pattern our proposed work will not yield significant improvement over standard CS based methods.

We have shown that the correlation among the different T2 weighted images of the same anatomical cross section can be used to formulate a group sparsity promoting optimization problem. Our proposed technique yields significant improvement in the reconstruction results. We carried out thorough experimentation on ex-vivo and in-vivo T2 weighted images of a rat's spinal cord.

The final goal of multi-echo T2 imaging is to compute the T2 map of the anatomical slice. Image reconstruction is the most crucial intermediate step. When the reconstructed MR images are correct the T2 maps can be computed with high accuracy. In this work, we have shown this empirically by constructing the T2 maps of ex-vivo and in-vivo data of rat's spinal cord from MR images reconstructed by different CS based techniques.

Acknowledgment

We are thankful to Henry S. Chen of the UBC Highfield MRI center for providing the raw data and generating the T2 maps.

References

[1] M. Lustig, D.L. Donoho, J.M. Pauly, Sparse MRI: the application of Compressed Sensing for rapid MR imaging, Magnetic Resonance in Medicine 58 (6) (2007) 1182–1195.
[2] D.J. Holland, D.M. Malioutov, A. Blake, A.J. Sederman, L.F. Gladden, Reducing data acquisition times in phase-encoded velocity imaging using compressed sensing, Journal of Magnetic Resonance 203 (2) (2010) 236–246.
[3] M. Doneva, P. Börnert, H. Eggers, C. Stehning, J. Sénégas, A. Mertins, Compressed sensing reconstruction for magnetic resonance parameter mapping, Magnetic Resonance in Medicine 64 (4) (2010) 1114–1120.
[4] K.T. Block et al., Model-based iterative reconstruction for radial fast spin-echo MRI, IEEE Transactions in Medical Imaging 28 (2009) 1759–1769.
[5] J. Trzasko, A. Manduca, Highly undersampled magnetic resonance image reconstruction via homotopic l0-minimization, IEEE Transactions in Medical Imaging 28 (1) (2009) 106–121.
[6] S. Hu, M. Lustig, A.P. Chen, J. Crane, A. Kerr, D.A.C. Kelley, R. Hurd, J. Kurhanewicz, S.J. Nelson, J.M. Pauly, D.B. Vigneron, Compressed sensing for resolution enhancement of hyperpolarized 13C flyback 3D-MRSI, Journal of Magnetic Resonance 192 (2) (2008) 258–264.
[7] R.N. Strickland, H.I. Hee, "The wavelet transform as a multiresolution matched filter and zero-crossing detector for detecting microcalcifications in mammograms", Engineering in Medicine and Biology (1995) 1047–1048.
[8] E.J. Candès, J. Romberg, T. Tao, Robust uncertainty principles: exact signal reconstruction from highly incomplete frequency information, IEEE Transactions on Information Theory 52 (2) (2006) 489–509.
[9] Y.C. Eldar, P. Kuppinger, H. Bolcskei, Block-sparse signals uncertainty relations and efficient recovery, IEEE Transactions on Signal Processing 58 (6) (2010) 3042–3054.
[10] M. Stojnic, F. Parvaresh, B. Hassibi, On the Reconstruction of Block-sparse Signals with an Optimal Number of Measurements, arXiv:0804.0041v1
[11] J. Huang, T. Zhang, The Benefit of Group Sparsity, arXiv:0901.2962v2.
[12] A. Majumdar, R.K. Ward, Compressive color sensing of color images, Signal Processing 90 (12) (2010) 3122–3127.
[13] E. van den Berg, M.P. Friedlander, Theoretical and empirical results for recovery from multiple measurements, IEEE Transactions in Information Theory 56 (5) (2010) 2516–2527.
[14] F.J. Herrmann, Compressive Imaging by Wavefield Inversion with Group Sparsity, SEG, Technical Report TR-2009-01, Houston, 2009.
[15] <http://www.cs.ubc.ca/labs/scl/spgl1/index.html>.
[16] R.G. Baraniuk, V. Cevher, M.F. Duarte, C. Hegde, Model-based Compressive Sensing, arXiv:0808.3572v5.
[17] I.W. Selesnick, M.A. Figueiredo, Signal restoration with overcomplete wavelet transforms: comparison of analysis and synthesis priors, in: Proceedings of SPIE, vol. 7446, Wavelets XIII, 2009.
[18] A. Majumdar, R.K. Ward, Under-determined Non-cartesian MR Reconstruction, MICCAI 2010, Beijing, China, 2010 (September 20–23).
[19] G. Hennenfent, E. van den Berg, M.P. Friedlander, F.J. Herrmann, New insights into one-norm solvers from the pareto curve, Geophysics 73 (4) (2008).
[20] T. Lin, F.J. Herrmann, Compressed extrapolation, Geophysics 72 (5) (2007) 77–93.
[21] P. Parasoglou, D. Malioutov, A.J. Sederman, J. Rasburn, H. Powell, L.F. Gladden, A. Blake, M.L. Johns, Quantitative single point imaging with compressed sensing, Journal of Magnetic Resonance 201 (1) (2009) 72–80.